

Gene cluster conservation identifies melanin and perylenequinone biosynthesis pathways in multiple plant pathogenic fungi

Malaika K. Ebert ^{1,2,3†} Rebecca E. Spanner ^{1,2†}
Ronnie de Jonge ^{4,5,6†*} David J. Smith,¹
Jason Holthusen,¹ Gary A. Secor,²
Bart P. H. J. Thomma ³ and Melvin D. Bolton ^{1,2**}

¹Red River Valley Agricultural Research Center, USDA Agricultural Research Service, Fargo, ND, USA.

²Department of Plant Pathology, North Dakota State University, Fargo, ND, USA.

³Laboratory of Phytopathology, Wageningen University, Wageningen, The Netherlands.

⁴Plant-Microbe Interactions, Department of Biology, Science4Life, Utrecht University, Utrecht, The Netherlands.

⁵Department of Plant Biotechnology and Bioinformatics, Ghent University, Ghent, Belgium.

⁶VIB Center for Plant Systems Biology, Ghent, Belgium.

Summary

Perylenequinones are a family of structurally related polyketide fungal toxins with nearly universal toxicity. These photosensitizing compounds absorb light energy which enables them to generate reactive oxygen species that damage host cells. This potent mechanism serves as an effective weapon for plant pathogens in disease or niche establishment. The sugar beet pathogen *Cercospora beticola* secretes the perylenequinone cercosporin during infection. We have shown recently that the cercosporin toxin biosynthesis (CTB) gene cluster is present in several other phytopathogenic fungi, prompting the search for biosynthetic gene clusters (BGCs) of structurally similar perylenequinones in other fungi. Here, we report the identification of the elsinochrome and phleochrome BGCs of *Elsinoë fawcettii* and *Cladosporium phlei*, respectively, based on gene cluster conservation with the CTB and hypocrellin BGCs.

Furthermore, we show that previously reported BGCs for elsinochrome and phleochrome are involved in melanin production. Phylogenetic analysis of the corresponding melanin polyketide synthases (PKSs) and alignment of melanin BGCs revealed high conservation between the established and newly identified *C. beticola*, *E. fawcettii* and *C. phlei* melanin BGCs. Mutagenesis of the identified perylenequinone and melanin PKSs in *C. beticola* and *E. fawcettii* coupled with mass spectrometric metabolite analyses confirmed their roles in toxin and melanin production.

Introduction

Fungi produce a plethora of secondary metabolites (SMs) that serve to enhance competitiveness in nature. Functional diversity of these compounds is high, including reported roles in virulence, biotic and abiotic stress protection and as metal transport agents (Williams *et al.*, 1989; Demain and Fang, 2000; Rohlf and Churchill, 2011; Stergiopoulos *et al.*, 2012; Keller, 2015). For example, in some occasions SMs are involved in symbiotic relationships where microbial symbionts provide an antibiotic armoury against secondary infection to the symbiotically colonized plant in return for nutrients and protection (Rohlf and Churchill, 2011; Stringlis *et al.*, 2018). A major class of fungal SMs are the polyketides (Keller *et al.*, 2005). For the biosynthesis of fungal aromatic polyketides, nonreducing polyketide synthases (NR-PKSs) play a central role as mediators of the first biosynthetic step (Keller *et al.*, 2005; Crawford and Townsend, 2010; Brakhage, 2013; Gallo *et al.*, 2013). Such PKS genes contain multiple domains that work conjointly, of which the β -ketoacyl synthase (Guedes and Eriksson, 2007), acyltransferase (AT) and acyl-carrier protein (ACP) domain are indispensable (Kroken *et al.*, 2003; Keller *et al.*, 2005; Crawford and Townsend, 2010; Gallo *et al.*, 2013). By using the domains iteratively, a PKS generates a metabolite backbone which can be modified by other enzymes to yield the final metabolite (Keller *et al.*, 2005; Bohnert *et al.*, 2010; Crawford and Townsend, 2010).

Received 24 April, 2018; accepted 5 November, 2018. For correspondence. *E-mail r.dejonge@uu.nl. **E-mail melvin.bolton@ars.usda.gov; Tel. +31(0)302536860. †These authors contributed equally to this work.

The genes encoding these decorating enzymes are often found in direct proximity to the PKS gene to form a biosynthetic gene cluster (BGC) pathway (Keller and Hohn, 1997; Keller *et al.*, 2005). In addition, BGCs often contain regulatory elements and transporters involved in shuttling the final secondary metabolite from the cell, and in the case of toxic metabolites, genes encoding auto-resistance proteins (Keller, 2015; de Jonge *et al.*, 2018).

A well-studied BGC is the cercosporin toxin biosynthesis (*CTB*) pathway. The *CTB* gene cluster was originally identified in *Cercospora nicotianae*, causal agent of leaf spot disease on tobacco, but is present in almost all *Cercospora* species (Assante *et al.*, 1977; Choquer *et al.*, 2005; de Jonge *et al.*, 2018). The ubiquitous presence of the *CTB* gene cluster in the genus is likely explained by its role as a virulence facilitator (Callahan *et al.*, 1999; Daub and Ehrenshaft, 2000; Choquer *et al.*, 2005). Recently, de Jonge and colleagues (2018) used comparative genomics to show that the *CTB* gene cluster can also be found in several plant pathogenic fungal species outside the *Cercospora* genus, likely as a result of horizontal transfer of the entire *CTB* gene cluster (Bohnert *et al.*, 2010; Crawford and Townsend, 2010; de Jonge *et al.*, 2018). The majority of assessed species from the genus *Colletotrichum*, a large genus of crop and/or ornamental plant pathogens (Perfect *et al.*, 1999), were shown to harbour full- to partial-length *CTB* gene clusters, of which the post-harvest apple fruit pathogen *Co. fioriniae* was shown to produce cercosporin (de Jonge *et al.*, 2018). The core gene of the *Cercospora CTB* gene cluster is the NR-PKS gene *CTB1* (Newman and Townsend, 2016), which is flanked by nine genes that encode decorating enzymes (*CTB2*, *CTB3*, *CTB5*, *CTB6*, *CTB7*, *CTB9*, *CTB10*, *CTB11* and *CTB12*) (de Jonge *et al.*, 2018). Besides those 10 genes essential for toxin formation, the cluster also encodes a zinc finger transcription factor (*CTB8*) for regulation of cluster gene expression, and two major facilitator superfamily (MFS) transporters; *CTB4* that is necessary for toxin secretion and the cercosporin facilitator protein (CFP) involved in toxin auto-resistance (Chen *et al.*, 2007; Choquer *et al.*, 2007; de Jonge *et al.*, 2018). Upon activation, all *CTB* pathway enzymes work in a well-orchestrated manner to synthesize the metabolite from backbone formation to secretion of the toxin into the environment while providing the fungus with protection against cercosporin.

Cercosporin is a member of the perylenequinone family that, upon photo-activation, displays almost universal toxicity to a wide spectrum of organisms (Zhenjun and Lown, 1990; Daub and Ehrenshaft, 2000; Ahonsi *et al.*, 2005; Guedes and Eriksson, 2007; Daub *et al.*, 2013). Exposure to visible and near-UV light energetically activates perylenequinones to an excited triplet state that reacts with oxygen to form reactive oxygen

species (Foote, 1976; Guedes and Eriksson, 2007). This photodynamic activity can be attributed to the 3,10-dihydroxy-4,9-perylenequinone chromophore backbone that is shared among perylenequinones (Hudson *et al.*, 1997). Structural differences between perylenequinone family members are mostly due to divergent side chains attached to the mutual backbone structure (Daub *et al.*, 2005) (Fig. 1). For example, the methylenedioxy bridge is a unique feature of cercosporin and is absent in other perylenequinones such as hypocrellin, elsinochrome and phleiochrome (Fig. 1) (Weiss *et al.*, 1987; de Jonge *et al.*, 2018).

Previous studies have implicated PKS genes in the production of perylenequinones in other plant pathogenic fungi. For example, transcriptome analysis and a CRISPR-Cas9 gene editing approach in the bamboo pathogen *Shiraia bambusicola* gave compelling evidence that *SbaPKS* encodes the PKS orchestrating hypocrellin biosynthesis (Zhao *et al.*, 2016; Deng *et al.*, 2017). Similarly, targeted disruption of *EfPKS1* in the citrus scab pathogen *Elsinoë fawcettii* abrogated elsinochrome production (Liao and Chung, 2008). Likewise, *Cppks1* was found to be responsible for PKS activity for phleiochrome production in the purple eyespot pathogen *Cladosporium phlei* based on homology to *EfPKS1* (So *et al.*, 2015). Our previous phylogenetic analysis of PKSs revealed that *EfPKS1* clusters with melanin biosynthesis PKSs and is relatively distant from *CTB1* (de Jonge *et al.*, 2018), corroborating previous findings by Liao and Chung (2008). Correspondingly, annotated *EfPKS1* flanking genes showed high similarity to established melanin biosynthesis genes, whereas *SbaPKS* flanking genes for hypocrellin biosynthesis resembled those found in the *CTB* cluster. Melanin is an integral component of the cell wall that has proposed functions in protection from environmental factors, appressorial penetration of host plants and pathogenesis (Wheeler and Bell, 1988; Langfelder *et al.*, 2003; Liu and Nizet, 2009). In *Mycosphaerella fijiensis*, research suggested that secreted fungal DHN-melanin acts as a virulence factor through the photogeneration of singlet molecular oxygen in a similar manner to the perylenequinones (Beltrán-García *et al.*, 2014). DHN-melanin biosynthesis has been characterized extensively in many fungi, including *Magnaporthe oryzae*, *Colletotrichum lagenarium*, *Alternaria alternata*, *Botrytis cinerea*, *Verticillium dahliae* and *Aspergillus* spp. In the rice blast fungus *M. oryzae* for instance, DHN-melanin production is known to be mediated by a four-gene cluster which is regulated in hyphae by the transcription factor Pig1 (Supporting Information Fig. 1) (Thompson *et al.*, 2000; Tsuji *et al.*, 2000; Talbot, 2003; Oh *et al.*, 2008). However, fungal DHN-melanin pathways may vary in the biosynthesis of the first common intermediate 1,3,6,8-tetrahydroxynaphthalene (1,3,6,8-THN or T4HN). For example, the PKS ALB1 (for 'albino 1') is

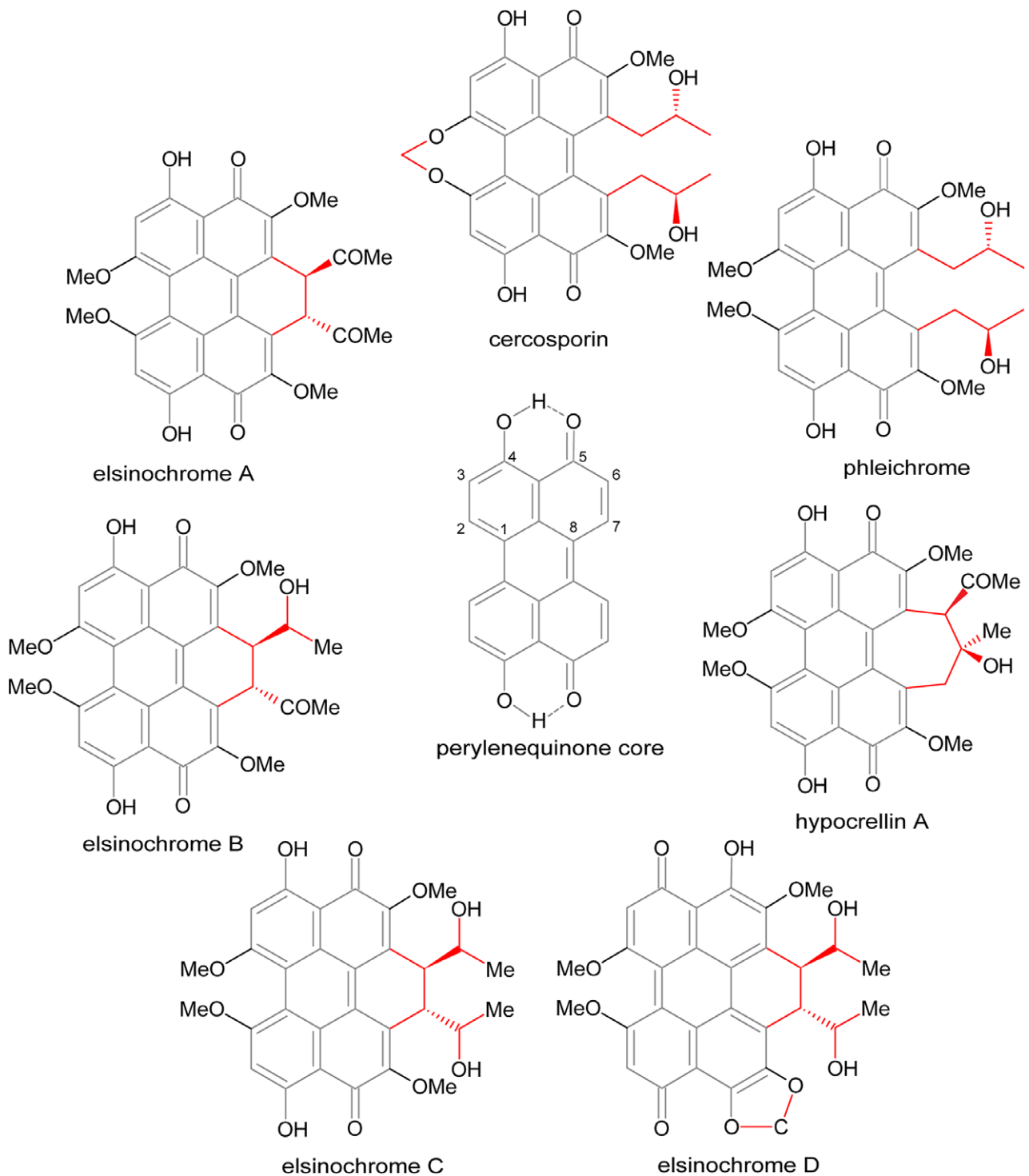


Fig. 1. Structures of related perylenequinones.

Cercosporin synthesized by *Cercospora* spp., phleichrome by *C. phlei*, hypocrellin A by *S. bambusicola* and elsinochromes A, B, C and D produced by *E. fawcettii* are structurally related as they share a common perylenequinone core (center; indicated in the molecule structure in grey). Structural differences between the molecules are mostly due to various side chains (indicated in red). Differences between perylenequinones are observed at positions 2, 2' and 7, 7'. [Color figure can be viewed at wileyonlinelibrary.com]

responsible for the first biosynthetic step in *Aspergillus fumigatus*, resulting in the biosynthesis of the heptaketide naphthopyrone YWA1, which is subsequently hydrolyzed

by Ayl1 to produce T4HN (Fujii *et al.*, 2004; Pihet *et al.*, 2009). Two alternative routes can be found in the necrotrophic grey mould fungus *B. cinerea*. In this case, the

PKSs Bcpks12 and Bcpks13 synthesize different precursors for the joint DHN-melanin pathway (Schumacher, 2016). While Bcpks12 produces the pentaketide T4HN directly, Bcpks13 synthesizes the hexaketide 2-acetyl-1-,3,6,8-tetrahydroxynaphthalene (AT4HN) that is subsequently converted to yield T4HN (Schumacher, 2016). In either case, the resulting T4HN will serve as substrate for a hydroxynaphthalene (HN) reductase leading to scytalone formation. In the next step, scytalone will be dehydrated by a scytalone dehydratase resulting in the formation of 1,3,8-trihydroxynaphthalene (1,3,8-THN or T3HN). Subsequent reduction by a HN reductase yields vermeline which is subsequently dehydrated to form 1,8-DHN; an immediate precursor of melanin (Tsai *et al.*, 1999; Thompson *et al.*, 2000; Tsuji *et al.*, 2000; Talbot, 2003).

Here, we set out to prepare draft genome sequences for *E. fawcettii* and *C. phlei* to unravel the evolutionary trajectories of both melanin and perylenequinone BGCs. We show that the gene clusters housing *Cpks1* and *EfPKS1* have high similarity to established gene clusters involved in DHN-melanin biosynthesis and have only limited similarity to the perylenequinone biosynthesis clusters to which they were previously attributed. Consequently, we also sought to establish the BGCs involved in production of elsinochrome in *E. fawcettii* and phleichrome in *C. phlei* using targeted gene replacement of both perylenequinone and melanin PKS genes in *E. fawcettii* and *C. beticola* to provide proof for their involvement in toxin and DHN-melanin production.

Results

E. fawcettii and *C. phlei* genomics

To initiate our investigation on perylenequinone and melanin BGCs of *E. fawcettii* and *C. phlei*, we developed draft genome sequences of both species. Nuclear and mitochondrial DNA of *E. fawcettii* strain CBS 139.25 and *C. phlei* strain CBS 358.69 were sequenced to approximately 138-fold and 110-fold coverage, respectively, on the Illumina HiSeq 4000 platform (paired-end, 100-bp reads). Reads were *de novo* assembled by SPAdes yielding draft genome assemblies of 25.3 Mb on 398 scaffolds for *E. fawcettii* and 31.9 Mb on 794 scaffolds for *C. phlei*. The, respective, scaffold N50 values and L50 numbers for these assemblies are 13 and 676 Kb, and 44 and 238 Kb. Following genome assembly, we used Augustus to predict 9519 and 11,316 protein-coding genes for *E. fawcettii* and *C. phlei* respectively.

PKS genealogy and prediction of function

To study the level of conservation of PKSs and associated pathways involved in the biosynthesis of different perylenequinones, we mined the genomes of both perylenequinone

producers and nonproducers for nonreducing PKSs (Supporting Information Table 1). Subsequently, the phylogenetic relationships between these PKSs and those of previously characterized PKSs from selected species (Collemare *et al.*, 2014) (Supporting Information Table 1) were determined by aligning the highly conserved KS (Guedes and Eriksson, 2007) domains of each PKS (Fig. 2). This KS genealogy revealed distinctive clade formation where PKSs with confirmed involvement in biosynthesis of structurally similar metabolites were observed to cluster. The clades were categorized as perylenequinone, aflatoxin, anthraquinone or DHN-melanin biosynthesis depending on the function of confirmed PKSs they harboured (Fig. 2). Interestingly, the PKSs *EfPKS1* (Liao and Chung, 2008)/[ELSAW09157-RA (this study)] from *E. fawcettii* and *Cpks1* (So *et al.*, 2015)/[CLAPH08786-RA (this study)] from *C. phlei* that were previously implicated in perylenequinone biosynthesis did not cluster phylogenetically with the established perylenequinone cercosporin PKSs CbCTB1 and CnCTB1 of *C. beticola* and *C. nicotianae* respectively. Instead, *EfPKS1* and *Cpks1* formed a clade with confirmed melanin PKSs, including Bcpks12 and Bcpks13 of the grey mould fungus *B. cinerea* (Schumacher, 2016), *Wdpks1* of the zoopathogenic black yeast *Wangiella (Exophiala) dermatitidis* (Feng *et al.*, 2001), *GIPKS1* of the filamentous fungus *Glarea lozoyensis* (Zhang *et al.*, 2003), *NodPKS1* of an endophytic *Nodulisporium* strain (Fulton *et al.*, 1999), *COGPKS1* of the cucumber anthracnose causal agent *Co. lagenarium* (Fujii *et al.*, 1999), the predicted *C. beticola* melanin biosynthesis PKS CbPKS1 (CBET3_09638) and the *S. bambusicola* melanin PKS SHIR08477. The finding that *E. fawcettii* ELSAW09157-RA, *C. phlei* CLAPHL08786-RA, *S. bambusicola* SHIR08477 and *CbPKS1* reside in a cluster (Fig. 2) with extensive collinearity to established DHN-melanin clusters (Fig. 3) suggests a role in melanin production and hints that *EfPKS1* and *Cpks1* were previously misannotated as perylenequinone biosynthesis genes (Liao and Chung, 2008; So *et al.*, 2015).

The cercosporin PKSs in *C. beticola* (CbCTB1), *C. nicotianae* (CnCTB1) and *Co. fiorinae* (EXF84093) form a perylenequinone clade with the previously confirmed hypocrellin PKS (SbaPKS) (Zhao *et al.*, 2016; Deng *et al.*, 2017), ELSAW08003 from *E. fawcettii*, CLAPHL05460 from *C. phlei* as well as with the putative elsinochrome PKS in *P. nodorum* (EAT83782.2) (Chooi *et al.*, 2017), the putative perylenequinone PKS *M. oryzae* (MGG_00428) and the *C. beticola* CbCTB1 paralog CBET3_10910 (Fig. 2). As phylogenetic conservation can be an indication of related metabolite production (de Jonge *et al.*, 2018), this clustering suggests that PKSs of this clade are involved in biosynthesis of the perylenequinones. Therefore, we suggest renaming ELSAW08003 to *EfETB1* for elsinochrome toxin

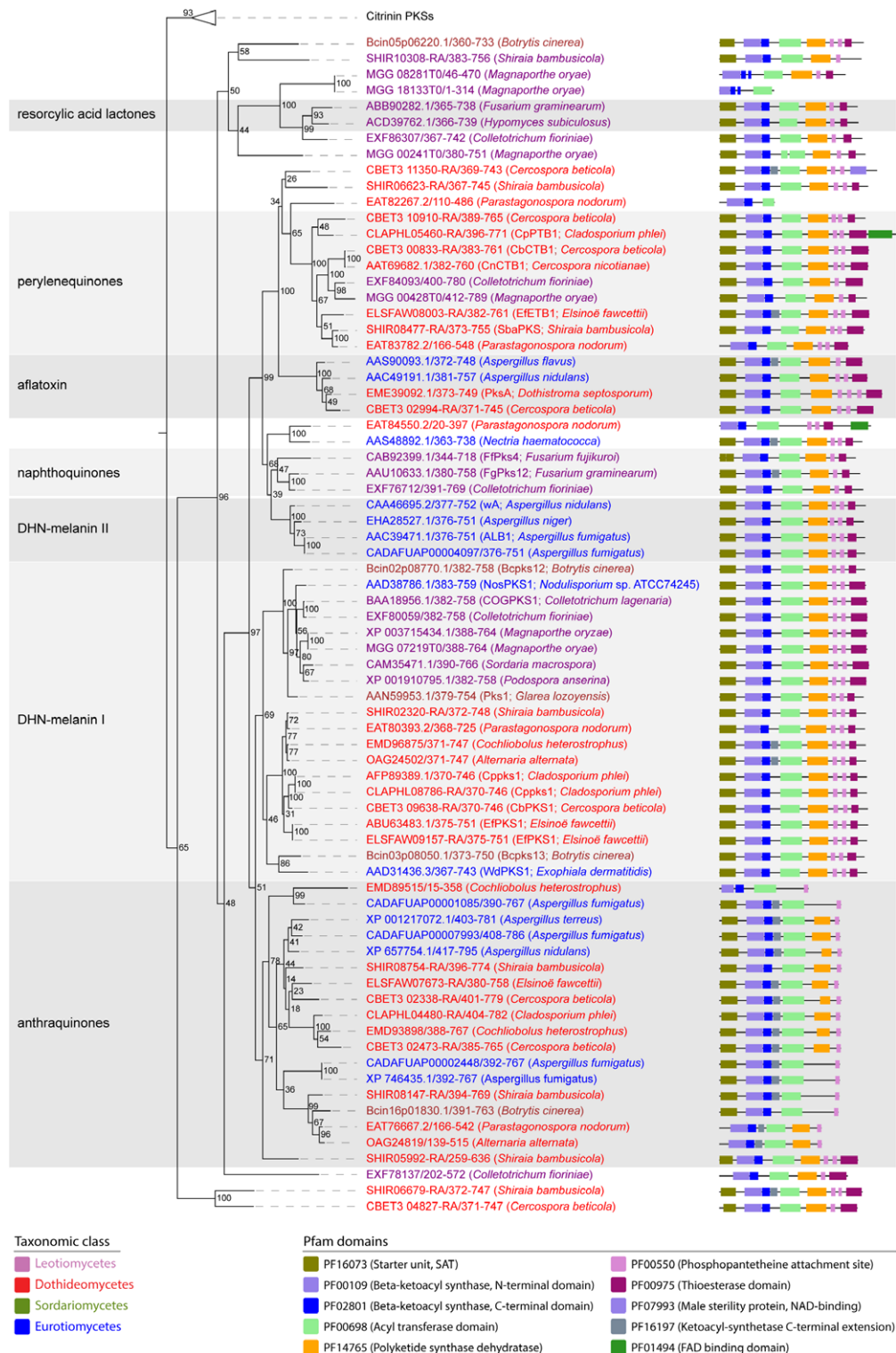


Fig. 2. Phylogeny of PKSs of related Ascomycetes revealing distinct DHN-melanin and perylenequinone clades.

Maximum likelihood phylogenetic tree illustrating the phylogenetic relationship of all predicted nonreducing polyketide synthases (PKSs) from the selected species set (Supporting Information Table 1) plus those derived from the set of PKSs used by Collemare and colleagues (2014). The tree was constructed from the aligned full-length β -ketoacyl synthase (Guedes and Eriksson, 2007) domains. The right panel indicates domain architecture of each PKS determined by Pfam domain annotation. Protein accessions are coloured depending on the taxonomic class of the producing species, and the species identifier can be found in the taxa labels. Established biosynthetic end products for a subset of the listed PKSs is indicated by the background colour, highlighting two DHN-melanin sub-groups, naphthoquinones, anthraquinones, perylenequinones, aflatoxin-like compounds and resorcylic acid lactones. [Color figure can be viewed at wileyonlinelibrary.com]

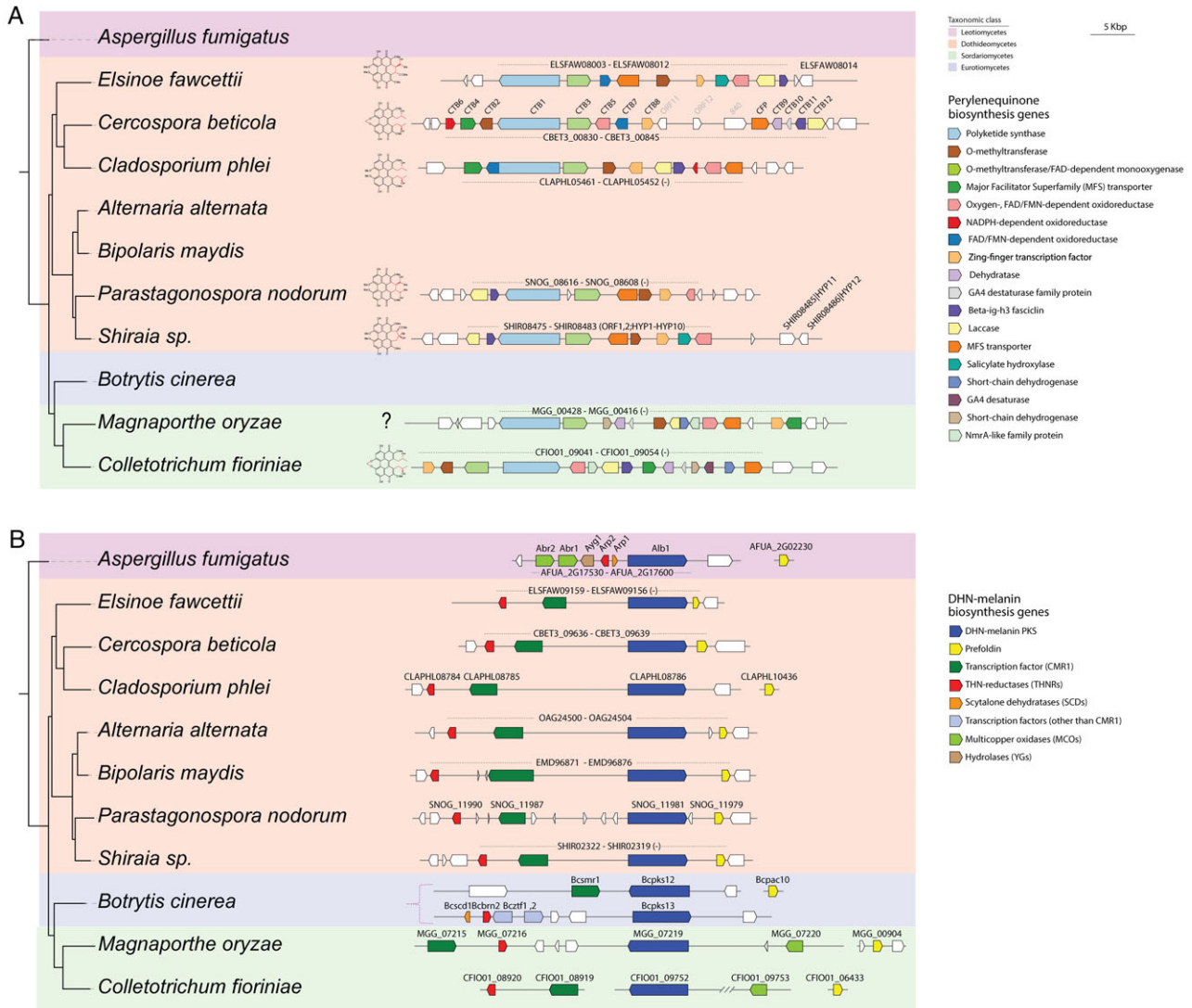


Fig. 3. Synteny and rearrangements of conserved perylenequinone and DHN-melanin BGCs. **A.** Alignment of established and putative perylenequinone BGCs of *E. fawcettii*, *C. beticola*, *C. phlei*, *P. nodorum*, *S. bambusicola*, *M. oryzae* and *Co. fioriniae*. Structural differences between different perylenequinone molecules are highlighted in red. For *E. fawcettii*, the elsinochrome B molecule structure is representative for elsinochromes A to D, cercosporin has been identified to be produced by *C. beticola* and *Co. fioriniae* while phleiochrome is known to be secreted by *C. phlei* and hypocrellin A was shown to be one of the perylenequinones secreted by *S. bambusicola*. **B.** DHN-melanin BGC alignment of putative and established DHN-melanin BGCs of *E. fawcettii*, *C. beticola*, *C. phlei*, *P. nodorum*, *S. bambusicola*, *M. oryzae*, *Co. fioriniae*, *A. fumigatus*, *A. alternata*, *B. maydis* (*C. heterostrophus*) and *B. cinerea*. The phylogenetic tree of Ascomycetes used in this study was constructed based on mash protein-level kmer hash overlaps. Alignment plots were prepared with MultiGeneBlast. For all species, the indicated identifiers are transcript IDs and the corresponding sequences can be retrieved from Ensemble Fungi and/or NCBI GenBank. *CTB* orthologs are coloured relative to the *C. beticola CTB* cluster genes while DHN-melanin BGC genes are colour coded relative to *M. oryzae* DHN-melanin. Colour key and annotated functions are explained in the legend next to the alignment plots. *E. fawcettii* and *S. bambusicola* genes, unrelated to previously annotated genes in the cercosporin BGC remain in white but are labelled by gene identity. [Color figure can be viewed at wileyonlinelibrary.com]

biosynthesis 1, and *C. phlei* CLAPHL05460 to *CpPTB1* for phleiochrome toxin biosynthesis 1.

Perylenequinone and DHN-melanin biosynthesis gene cluster alignments

While *PKS* genes are indispensable for polyketide formation, it is the full complement of genes in a BGC that is responsible for the biosynthesis of the end product.

Therefore, synteny of the predicted BGCs of orthologous *PKS* genes was assessed. Using the established *C. beticola CTB* gene cluster and *S. bambusicola* hypocrellin gene cluster as references, putative perylenequinone orthologous gene clusters in *E. fawcettii*, *C. phlei*, *P. nodorum*, *M. oryzae* and *Co. fioriniae* were aligned (Fig. 3A). Although, there is evidence for gene loss and gain between the perylenequinone BGC alignments, multiple core genes are shared between cercosporin,

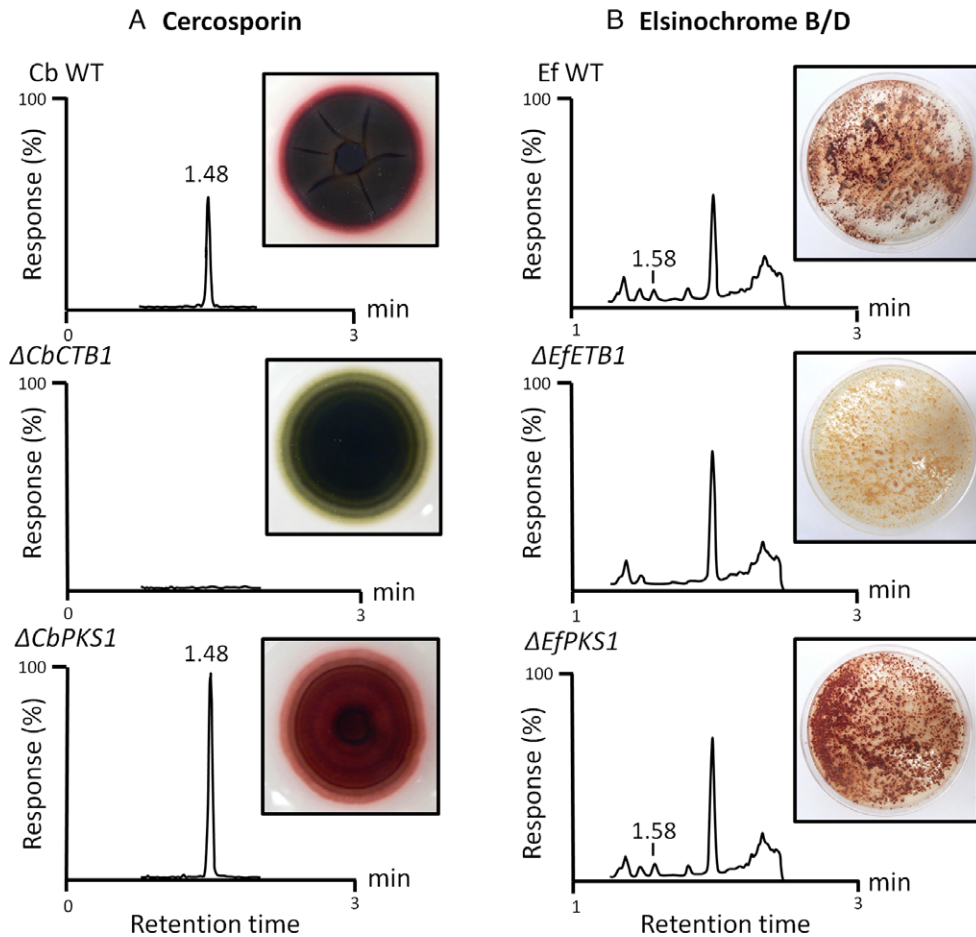


Fig. 4. Perylenequinone toxin detection in *C. beticola* and *E. fawcettii* wild types, and in perylenequinone and melanin PKS mutants. Representative ultra-performance liquid chromatography (UPLC) mass-selective detection of (A) cercosporin and (B) elsinochrome B/D are shown for each fungal strain (minimum of 2 plate extracts per strain). Cercosporin (column A) was present in *C. beticola* wild type and the $\Delta CbPKS1$ mutants at a retention time of 1.48 min, but not in the $\Delta CbCTB1$ mutants (the cercosporin standard produced a mass-selective chromatogram with an identical retention time; data not shown). An elsinochrome B/D peak (column B) was present in wild type *E. fawcettii* and $\Delta EfPKS1$ strains, retention time 1.58 min, and was undetectable in $\Delta EfETB1$ mutants (no chemical-grade standard available). [Color figure can be viewed at wileyonlinelibrary.com]

hypocrellin and the predicted BGCs for elsinochrome and phleichrome (Fig. 3A). Overall, eight genes are shared between the cercosporin, hypocrellin and predicted elsinochrome and phleichrome BGCs (Fig. 3A). When compared to these perylenequinone pathways, the *CTB* gene cluster encodes two additional proteins; a putative α -ketoglutarate-dependent dioxygenase (*CTB9*) and a candidate dehydratase (*CTB10*) that have been shown to be essential for the formation of the methylenedioxy bridge in cercosporin (de Jonge *et al.*, 2018). The predicted *C. phlei* phleichrome BGC contains all orthologous *C. beticola* *CTB* genes except for the above-mentioned *CTB9* and *CTB10*, in agreement with the lack of the methylenedioxy bridge in phleichrome. Likewise, the predicted *E. fawcettii* elsinochrome BGC lacks *CTB9* and *CTB10* as well as the cercosporin MFS transporter (*CTB4*) and the NADPH-dependent oxidoreductase (*CTB6*). Interestingly, the *E. fawcettii* BGC contains

ELSAW08009, which only has an ortholog in the hypocrellin gene cluster (*SHIR08482*) and in no other of the aligned BGCs (Fig. 3A). *ELSAW08009* and *SHIR08482* encode a putative salicylate hydroxylase based on sequence similarity to the conserved protein domain family TIGR03219 (*E*-value 2.98e-18), members of which are salicylate 1-monoxygenases. Besides sharing this gene with the elsinochrome pathway and lacking orthologs to *CTB9* and *CTB10*, the hypocrellin cluster also lacks *CTB* homologues *CTB4*, *CTB6* and *CTB7* compared to the cercosporin pathway (Fig. 3A). The elsinochrome BGC in *E. fawcettii* contains one additional gene encoding a MFS transporter with predicted association to perylenequinone biosynthesis, and comparably, the hypocrellin BGC in *Shiraia* sp. contains two additional genes that encode a MFS transporter and a short-chain dehydrogenase respectively. These genes were previously reported as *HYP11* and *HYP12* (KM434884.1) and were

differentially expressed in a hypocrellin-producing strain as compared to a nonproducer (Zhao *et al.*, 2016).

Similarly, predicted DHN-melanin clusters of *C. beticola*, *C. phlei*, *E. fawcettii*, *S. bambusicola* sp. *slf14* and *Co. fiorinae* were aligned to the established DHN-melanin cluster of *M. oryzae*, *A. fumigatus*, *A. alternata*, *Bipolaris maydis* (*Cochliobolus heterostrophus*) and both alternative clusters of *B. cinerea* (Fig. 4B). All BGCs share homologous PKS genes, a THN-reductase and a prefoldin-encoding gene. Prefoldins are frequently associated with DHN-melanin BGCs, but a functional role in DHN-melanin biosynthesis has not been established to date. Furthermore, the putative melanin clusters of *C. beticola*, *C. phlei*, *E. fawcettii*, *S. bambusicola* sp. *slf14* and *Co. fiorinae* encode a transcription factor with homology to *M. oryzae* Pig1 and *Co. lagenarium* CMR1, which are frequently observed in other established melanin clusters (Tsuji *et al.*, 2000).

Targeted replacement and characterization of perylenequinone and melanin PKS genes

The predicted perylenequinone and melanin PKS genes for *C. beticola* (*CbCTB1* and *CbPKS1* respectively) and *E. fawcettii* (*EfETB1* and *EfPKS1* respectively) were targeted for split marker gene replacement. At least two unique site-directed transformants were assessed for involvement in metabolite production. The wild type and all knockout mutant strains were grown under conditions to induce perylenequinone production. The presence or absence of cercosporin (*C. beticola*) and elsinochrome (*E. fawcettii*) in culture extracts was determined via UPLC-MS (Fig. 4A and B). For both fungal species, perylenequinone production was abrogated in the perylenequinone PKS mutants ($\Delta CbCTB1$ and $\Delta EfETB1$ mutants for *C. beticola* and *E. fawcettii* respectively) but not in the melanin PKS mutants (Fig. 4A and B). There were no obvious differences in growth rate for either of the *C. beticola* or *E. fawcettii* mutants versus the corresponding wild type strains. Additionally, $\Delta CbPKS1$ and $\Delta EfPKS1$ melanin mutants had a pale buff colour as opposed to the dark grey pigmentation observed in wild type and perylenequinone-deficient mutant ($\Delta CbCTB1$ and $\Delta EfETB1$ for *C. beticola* and *E. fawcettii* respectively) strains (Fig. 5A and B). The amount of melanin present in the *C. beticola* and *E. fawcettii* cultures was determined spectrophotometrically. In both species, the $\Delta PKS1$ mutant had a significantly lower melanin content than either the wild type or $\Delta CbCTB1/\Delta EfETB1$ (Fig. 5C).

Discussion

Phylogenetic analysis based on PKS KS domain conservation can help to predict SM structure and gene

evolution (Keller *et al.*, 2005; Gallo *et al.*, 2013). In this study, we used KS domain sequence alignments and phylogenetic analysis of selected plant pathogenic fungi to separate PKSs into distinct clades. One of the clades hosted PKSs involved with perylenequinone biosynthesis including *CbCTB1*, the well-studied *C. beticola* PKS essential for cercosporin biosynthesis, and the PKS of the hypocrellin pathway in *S. bambusicola* sp. *slf14*. We also observed clustering of PKSs involved in DHN-melanin formation such as *Bcpks12* and *Bcpks13* of *B. cinerea* and *COGPKS1* of *Co. lagenarium* (Fig. 2). As previously reported (Liao and Chung, 2008), phylogenetic analyses of KS and AT domain sequences indicated a closer relationship of *EfPKS1* to melanin PKSs than to perylenequinone PKSs. Furthermore, high similarity of the full length amino acid sequence to the annotated *EfPKS1* led So and colleagues (2015) to hypothesize that *Cppks1* was involved in phleiochrome production. Our KS domain alignment confirms the phylogenetic analysis by Liao and Chung (2008) where *EfPKS1* and *Cppks1* form a cluster with established DHN melanin biosynthesis PKSs of other Ascomycetes (Fig. 2). Consequently, we used comparisons to well-characterized melanin BGCs in various Ascomycetes to show that PKSs belonging to the DHN-melanin clade are putatively involved with melanin biosynthesis in *C. beticola*, *E. fawcettii*, *C. phlei* and *S. bambusicola* sp. *slf14* (Fig. 3B). Whole-cluster homology of predicted cognate clusters to various well established DHN-melanin clusters strengthened our hypothesis that *CbPKS1*, *EfPKS1* and *Cppks1* are involved with melanin production.

To gain further support, we generated PKS mutants in our candidate melanin biosynthesis PKS genes in *C. beticola* and *E. fawcettii*. As predicted, the melanin null mutants $\Delta EfPKS1$ and $\Delta CbPKS1$ displayed pale phenotypes characteristic of previously described melanin-deficient mutant fungal strains (Chumley and Valent, 1990) (Fig. 5A and B). Additional quantitative determination of melanin in $\Delta CbPKS1$ of *C. beticola* and $\Delta EfPKS1$ of *E. fawcettii* indicated reduced melanin content of the culture compared to wild type and $\Delta CbCTB1$ or $\Delta EfETB1$ perylenequinone knockout mutant lines respectively (Fig. 5C and D). Interestingly, the *C. beticola* $\Delta CbPKS1$ and *E. fawcettii* $\Delta EfPKS1$ mutants were still able to produce cercosporin and elsinochrome, respectively (Fig. 4A and B), unlike the observation by Liao and Chung (2008) where $\Delta EfPKS1$ mutants in *E. fawcettii* were reported to be elsinochrome-deficient. Therefore, we suspect that the phenotype they observed may be due to *in vitro* conditions that were insufficient for perylenequinone induction. Previous functional analysis of the *EfPKS1* cluster raised questions when overexpression of predicted cluster genes under different conditions did not correlate with elsinochrome production and

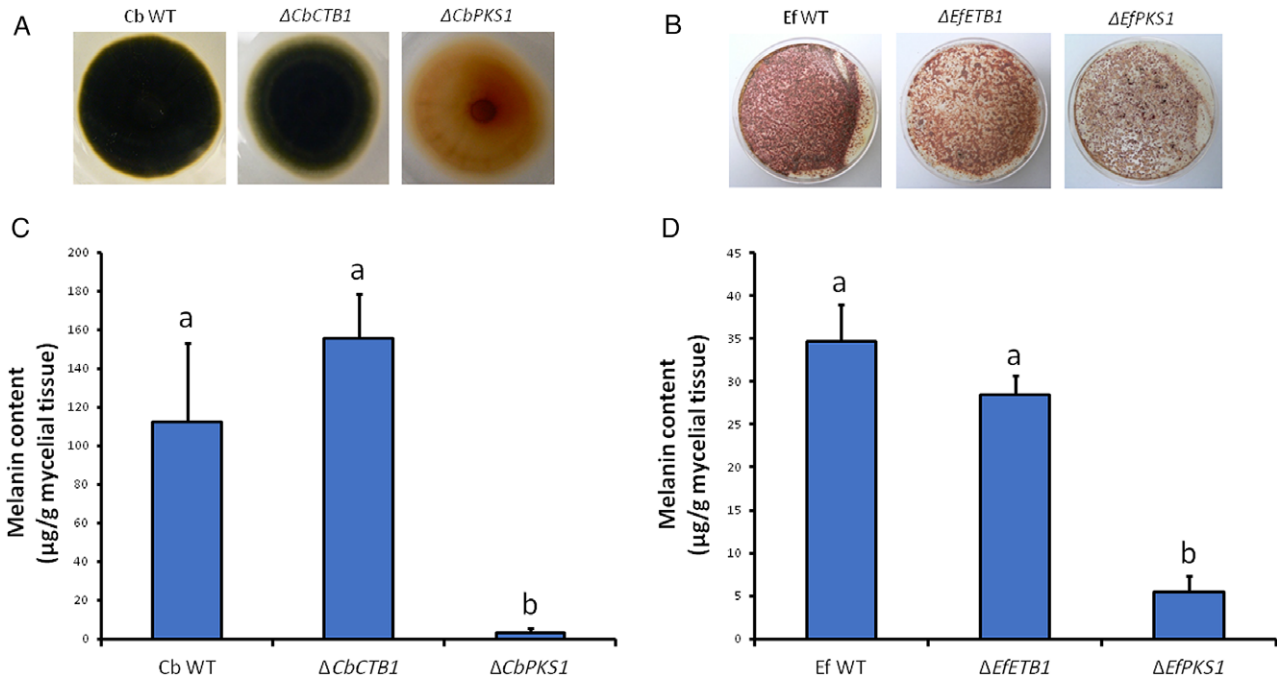


Fig. 5. Melanin production in *C. beticola* and *E. fawcettii* perylenequinone and melanin PKS mutants compared to wild type. Photos of (A) *C. beticola* and (B) *E. fawcettii* strains growing on CV8 agar in conditions conducive to melanin production (24-h light, 21°C). C. The mean melanin content of three individual fungal cultures (μg melanin/g of mycelial tissue ± standard error) in *C. beticola* wild type (WT), melanin mutants (ΔCbPKS1) and cercosporin mutants (ΔCbCTB1). D. *E. fawcettii* wildtype (WT), melanin mutants (ΔEfPKS1) and elsinochrome mutants (ΔEfETB1). Significant differences between strains are indicated by letters. [Color figure can be viewed at wileyonlinelibrary.com]

complementation of the transcription factor-like gene *EFTSF1* null mutant (with *EFTSF1*) was unable to restore elsinochrome production to wild type level (Chung and Liao, 2008). Here, putative Δ*EFTSF1* transformants were identified on the basis of elsinochrome deficiency, potentially dismissing any true site-directed mutants that were still able to produce elsinochrome (Chung and Liao, 2008). Therefore, it could be that their elsinochrome-deficient phenotype was evoked by off target T-DNA insertion. The reduction in virulence observed for their Δ*EfPKS1* mutant is not surprising as melanin has been reported to be a virulence factor for many filamentous fungi (Wheeler and Bell, 1988; Langfelder *et al.*, 2003; Liu and Nizet, 2009). Besides contribution to fungal virulence, melanin has also been reported to play an important role in protection against environmental stresses. Recently, studies of the causal agent of Septoria tritici blotch on wheat, *Zymoseptoria tritici*, have indicated a correlation between fungicide resistance and melanization level of the producing fungus which led to the identification of the putative *Z. tritici* melanin PKS (Lendenmann *et al.*, 2014; Lendenmann *et al.*, 2015). Similarly, *CbPKS1* and *CBET3_09636*, encoding a predicted tetrahydroxynaphthalene (T4HN) reductase (now renamed to *Cb4HNR* as it is homologous to *4HNR* of *M. oryzae*), that we propose to belong to the melanin BGC have been

recently reported to be more highly expressed in fungicide-resistant *C. beticola* strains compared to fungicide-sensitive strains (Bolton *et al.*, 2016). Consequently, we propose that melanin production in *C. beticola* is mediated by *CbPKS1* which forms T4HN in the first biosynthetic step. Subsequently, T4HN will serve as substrate for *Cb4HNR* which reduces it to yield scytalone. Taken together, these results strongly suggest that *EfPKS1* and *CpPKS1* are involved in DHN-melanin biosynthesis, in contrast to earlier reports (Liao and Chung, 2008; So *et al.*, 2015).

To identify the legitimate elsinochrome and phlei-chrome PKS genes in *E. fawcettii* and *C. phlei*, respectively, we went back to our KS domain alignment where predicted PKSs CpPTB1 of *C. phlei* and EfETB1 of *E. fawcettii* clustered together with established cercosporin biosynthesis PKSs CTB1 in *C. beticola* and *C. nicotianae* (Fig. 2). In line with these initial functional predictions, alignments of the corresponding predicted gene clusters display high similarity and gene conservation within each clade (Fig. 3A). Also, structural differences between perylenequinones can be explained by comparing the predicted metabolite clusters on a gene level. For example, cercosporin and phleiochrome only differ in the additional methylenedioxy bridge that is found in the cercosporin molecule (Fig. 1). Accordingly, the

predicted phleochrome biosynthesis pathway lacks *CTB9* and *CTB10* that have been shown to be responsible for methylenedioxy bridge formation (de Jonge *et al.*, 2018). Site-directed gene replacement of *EfETB1* in *E. fawcettii* and *CbCTB1* in *C. beticola* led to the successful generation of perylenequinone mutants that are deficient in toxin production under perylenequinone-inducing conditions (Fig. 4A and B). Since SM production relies on different environmental conditions, not every medium is suitable to activate SM production (Calvo *et al.*, 2002; VanderMolen *et al.*, 2013). For *C. beticola*, previous research has shown that growth on 'thin' PDA plates under natural light stimulates cercosporin production (Frandsen, 1955; Fajola, 1978; Jenns *et al.*, 1989), which was shown here to stimulate elsinochrome production.

In conclusion, we have identified BGCs of structurally related SM compounds based on the phylogenetic relationship of their encompassing PKSs and overall conservation level of the associated cluster genes. By using an established *CTB* gene cluster as reference, it was possible to identify gene clusters responsible for the synthesis of related perylenequinone compounds in different fungal species. Likewise, we successfully identified clusters associated with DHN-melanin production in *C. beticola*, *E. fawcettii*, *C. phlei*, *P. nodorum* and *S. bambusicola* using the same approach and the confirmed DHN-melanin cluster as input. Future research using this methodology will be useful for the identification of other perylenequinones and their corresponding BGCs in other fungi.

Experimental procedures

Elsinoë fawcettii and *Cladosporium phlei* genome sequencing

For high-quality genomic DNA extraction of *Elsinoë fawcettii* strain CBS 139.25 and *Cladosporium phlei* strain CBS 358.69, mycelia was scraped from the surface of PDA agar petri dishes and extracted using the CTAB method (Bolton *et al.*, 2016). Library preparation (500 bp) and subsequent paired-end (PE) sequencing on the Illumina HiSeq 4000 platform was done by BGI Americas (BGI Americas, Cambridge NA). Approximately 34 million high-quality sequence reads with an average length of 100 bp were generated for both samples, representing 134- and 111-fold coverage for *E. fawcettii* and *C. phlei* respectively. Draft genomes were assembled using SPAdes (version 3.9.0), with default parameters and k-mers 21, 33, 55, 77 and 99. Prediction of protein-coding gene models was performed *ab initio* using the previously prepared *Cercospora beticola* training parameters (de Jonge *et al.*, 2018) in Augustus (version 3.2.1). Protein function and subcellular localization was predicted by

Interpro (Finn *et al.*, 2017). Genome sequences and annotations are available under BioProject PRJNA475685 and permanently linked on figshare under doi <https://doi.org/10.6084/m9.figshare.6173834>.

Secondary metabolite phylogenetic analyses

Phylogenetic analysis of the type I PKS genes and phylogenetic tree analyses were largely performed as described in de Jonge and colleagues (2018). In short, we used Pfam domain scanning analyses by HMMER3 (Mistry *et al.*, 2013) with hmm profiles for domains PF00109.25 (Beta-ketoacyl synthase, N-terminal domain) and PF02801.21 (Beta-ketoacyl synthase, C-terminal domain) to identify all PKSs in the predicted proteomes of *C. beticola* (09-40), *C. phlei* (CBS 358.69), *E. fawcettii* (CBS 139.25), *S. bambusicola* (Slf14), *P. nodorum* (SN15), *C. heterostrophus* (C5), *A. alternata* (SRC1lrK2f), *A. fumigatus* (Af293), *B. cinerea* (B05.10), *Co. fioriniae* (PJ7) and *M. oryzae* (70-15) that were obtained from NCBI GenBank or Ensemble Fungi. In total we identified 240 proteins across these 11 proteomes. In addition, we added 70 PKSs from Collemare and colleagues (2014) and Cppks1 (AFP89389.1) from So and colleagues (2015). All selected proteins for further analyses are listed in Supporting Information Table 1. All 311 PKS proteins were subsequently aligned by Mafft (v7.271) using default parameters, after which we extracted the KS domain proportion as previously defined by Pfam scanning. This resulted in an alignment with 311 proteins across 832 positions that was used to prepare a maximum likelihood phylogenetic tree using RAxML (version 8.2.11), incorporating 100 rapid bootstraps and subsequent automatic, thorough ML search. We then selected the subclass of 94 nonreducing PKSs for further analysis, as defined previously by Kroken and colleagues (2003). The final phylogenetic tree and figure was prepared in EvolView (Zhang *et al.*, 2012). In this tree, we collapsed the outgroup clade with 20 members containing PKSs involved with citrinin biosynthesis, as indicated in Fig. 2. Inclusion in the final set of 74 noncollapsed, nonreducing PKSs is indicated in Supporting Information Table 1.

Secondary metabolite cluster alignment visualization

For comparative analyses of the secondary metabolite clusters across multiple genome sequences we initially identified orthologous protein families across the aforementioned proteomes using orthoFinder (Emms and Kelly, 2015). Subsequently, we used the MultiGeneBlast algorithm (multigeneblast.sourceforge.net), integral part of antiSMASH (Weber *et al.*, 2015), to prepare gene-by-gene cluster alignments across all species and we then re-coloured individual genes within each gene cluster according to the protein family analysis.

Deletion mutant generation

Site-directed gene replacements of *CTB1* and *CbPKS1* in *C. beticola* strain 1–90 and of *EfETB1* and *EfPKS1* in *E. fawcettii* strain CBS 139.25 were generated using the split-marker approach as described in Bolton and colleagues (2016). Primers are listed in Supporting Information Table 2. Regardless of phenotype, all putative knock-out mutants were screened for site-directed gene replacement. Successful gene deletion was confirmed by the presence of a PCR product using a forward primer upstream of the 5' flanking region of the target gene design and hygromycin reverse primer MDB-1145 (Supporting Information Fig. 2). Additionally, absence of an amplicon using target gene-specific primers reconfirmed deletion of the target gene (Supporting Information Table 2).

Perylenequinone production assay

Mycelial plugs of 5 mm in diameter from PKS mutant and wild-type *C. beticola* and *E. fawcettii* strains were grown on thin potato dextrose agar (PDA, Difco™, BD Diagnostic Systems, Sparks) plates (3.0 ml PDA in a 50 mm Petri plate, amended with 150 µg/ml hygromycin B (Roche, Mannheim, Germany; for mutant strains) under a 16 h light-8 h dark cycle at 21°C for 7 days. Three 5 mm diameter mycelial plugs of each *E. fawcettii* strain were ground with a micro-pestle in 1 ml potato dextrose broth (PDB, Difco™, BD Diagnostic Systems, Sparks), spread onto thin PDA plates and were grown under 24 h light at 28°C for 7 days.

Total mycelial tissue was excised from the agar plate, blended at high speed for 20 s and extracted with ethyl acetate whilst stirring for 5 min in the dark. Single plate extracts were filtered using two layers of miracloth and dried under a stream of nitrogen (21°C). The reddish-brown residues were resuspended in 200 µl methanol. Cercosporin concentration was calculated by measuring absorbance at 255 nm using an Agilent Cary 8454 UV–Visible spectrophotometer (Agilent Technologies, Inc., Santa Clara) and 21, 500 as the molar extinction coefficient (Milat and Blein, 1995). Extracts were diluted to ~100 pg µl⁻¹ with methanol and centrifuged at 3000 x g for 5 min. At a minimum, duplicate plate extracts were submitted for mass spectrometric analyses of each fungal strain.

Mass spectrometric analyses

Positive mode electrospray ionization settings were optimized for cercosporin by infusing a methanolic cercosporin standard (5 ng/µl) (Sigma; St. Louis) into a Waters (Milford, MA) Acquity triple quadrupole mass spectrometer.

The precursor ion, product ions, optimum collision energies and cone voltage were determined by the AutoTune Wizard within the MassLynx 4.1 software (Waters; Milford, MA). Ion transitions used for cercosporin detection were *m/z* 535 → 415 and *m/z* 535 → 485 using a cone voltage of 60 and collision energies of 25 and 20 V respectively.

Elsinochrome standard was not available, therefore, an extract from wild type *E. fawcettii* was infused into the mass spectrometer and fragmentation of ions appearing at *m/z* 547 (the molecular mass of elsinochromes B & D) were optimized using the AutoTune Wizard within the MassLynx 4.1. Presumptive elsinochrome ion transitions used were *m/z* 547 → 487 and *m/z* 547 → 457 using a cone voltage of 60 and collision energies of 20 and 35 V respectively. In some elsinochrome analyses, the mass spectrometer was used as a single sector instrument to collect molecular ions at *m/z* 547 (elsinochromes B & D), *m/z* 545 (elsinochrome A) and *m/z* 549 (elsinochrome C). For both cercosporin and elsinochrome MS/MS experiments, the desolvation temperature was set at 500°C, and the source temperature was set at 150°C. Cone gas (N₂) flow was set at 50 l/h and desolvation gas flow was set at 800 l/h, whereas the collision gas (Ar) flow was 0.16 ml/min.

Cercosporin and elsinochrome (isomers B and D) were analysed using liquid chromatography–tandem mass spectrometry (LC–MS/MS) using a Waters (Milford, MA) Acquity UPLC and Acquity triple-quadrupole mass spectrometer. Data were acquired, processed and quantified using MassLynx 4.1 with Target Lynx systems. Aliquots of sample extracts (10 µl) were injected onto a 2.1 × 30 mm (1.7 µm) Acquity CSH C18 column protected by a 2.1 × 5 mm CHS guard column (Waters; Milford, MA). Cercosporin and elsinochrome were eluted with a binary gradient consisting of solvent A (0.1% formic acid in pure water) and solvent B (0.1% formic acid in acetonitrile) flowing at 1 ml/min. The gradient program was started at 95% A and transitioned to 25% A over 2 min, 5% A at 2.1 min and held at 5% A until 2.5 min when solvent A was ramped back to 95% A at 3 min. Solvent composition was held constant until the end of the run time at 4 min. The column temperature was 30°C.

Melanin production assay

Three mycelial plugs of 5 mm diameter from each of wild type and mutant *C. beticola* strains were ground with a micropestle in 1 ml V8 broth (10% (v/v) clarified V8 juice (Campbell's Soup Co., Camden), 0.5% (w/v) CaCO₃) and spread onto single Nylon membranes (Nytran® SuPer-Charge Nylon transfer membrane, Schleicher and Schuell, Keene, USA) overlaying V8 agar (as broth but with 1.5% (w/v) agar (BD, Franklin Lakes, USA)) plates (6 ml in a 50 mm Petri plate). *E. fawcettii* strains were

grown in the same way as *C. beticola* except for larger plate sizes (15 ml in a 90 mm Petri plate). *C. beticola* was grown under 24 h light at 21°C for 7 days and *E. fawcettii* for 10 days. Total mycelial tissue was excised and weighed before extracting melanin according to Gadd (1982). The tissue was boiled for 5 min in 10 ml distilled water, centrifuged and the pigment extracted from the supernatant by autoclaving with 3 ml of 1 M NaOH (20 min, 120°C). The extract was then acidified to pH 2 with concentrated HCl to precipitate melanin. The precipitate was washed three times with distilled water and dried under a stream of nitrogen (21°C).

Melanin extracts were solubilized in 2 ml of 2 M sodium hydroxide at 50°C. A spectrophotometric assay was used as described by Kauser and colleagues (2003) to measure melanin absorbance at 475 nm with a standard curve of synthetic melanin (Sigma-Aldrich, Milwaukee) from 1 to 100 µg per ml to determine melanin content. The mean melanin content was determined as micrograms of melanin per gram of mycelial tissue for three replicates (individual cultures) and the standard error of the mean calculated. One-way ANOVA was performed using a *P*-value of 0.05 as the significance threshold with a post hoc Tukey HSD test to determine differences between the mean melanin contents of wild type strains and each of the three mutants for *C. beticola* and *E. fawcettii*.

Acknowledgements

This project was supported in part by USDA-ARS CRIS project 3060-22000-044. Work in the laboratory of B.P.H.J.T. is supported by the Research Council Earth and Life Sciences (ALW) of the Netherlands Organization of Scientific Research (NWO). M.E. was supported by NWO grant 833.13.007. R.d.J. was financially supported by an EMBO Long-Term Fellowship (ALTF 359-2013) and a postdoctoral fellowship of the Research Foundation Flanders (FWO 12B8116N). We thank J. Neubauer (USDA – ARS) for excellent technical assistance. Mention of trade names or commercial products in this publication is solely for the purpose of providing specific information and does not imply recommendation or endorsement by the U.S. Department of Agriculture.

References

Ahonsi, M. O., Maurhofer, M., Boss, D., and Défago, G. (2005) Relationship between aggressiveness of *Stagonospora* sp. isolates on field and hedge bindweeds, and in vitro production of fungal metabolites cercosporin, elsinochrome a and leptosphaerodione. *Eur J Plant Pathol* **111**: 203–215.

Assante, G., Locci, R., Camarda, L., Merlini, L., and Nasini, G. (1977) Screening of the genus *Cercospora* for secondary metabolites. *Phytochemistry* **16**: 243–247.

Beltrán-García, M. J., Prado, F. M., Oliveira, M. S., Ortiz-Mendoza, D., Scalfó, A. C., Pessoa, A., Jr., et al. (2014)

Singlet molecular oxygen generation by light-activated DHN-melanin of the fungal pathogen *Mycosphaerella fijiensis* in black Sigatoka disease of bananas. *PLoS One* **9**: e91616.

Bohnert, M., Wackler, B., and Hoffmeister, D. (2010) Spotlights on advances in mycotoxin research. *Appl Microbiol Biotechnol* **87**: 1–7.

Bolton, M. D., Ebert, M. K., Faino, L., Rivera-Varas, V., de Jonge, R., Van de Peer, Y., et al. (2016) RNA-sequencing of *Cercospora beticola* DMI-sensitive and -resistant isolates after treatment with tetraconazole identifies common and contrasting pathway induction. *Fungal Genet Biol* **92**: 1–13.

Brakhage, A. A. (2013) Regulation of fungal secondary metabolism. *Nat Rev Microbiol* **11**: 21–32.

Callahan, T. M., Rose, M. S., Meade, M. J., Ehrenshaft, M., and Upchurch, R. G. (1999) CFP, the putative cercosporin transporter of *Cercospora kikuchii*, is required for wild type cercosporin production, resistance, and virulence on soybean. *Mol Plant Microbe Interact* **12**: 901–910.

Calvo, A. M., Wilson, R. A., Bok, J. W., and Keller, N. P. (2002) Relationship between secondary metabolism and fungal development. *Microbiol Mol Biol Rev* **66**: 447–459.

Chen, H.-Q., Lee, M.-H., and Chung, K.-R. (2007) Functional characterization of three genes encoding putative oxidoreductases required for cercosporin toxin biosynthesis in the fungus *Cercospora nicotianae*. *Microbiology* **153**: 2781–2790.

Chooi, Y.-H., Zhang, G., Hu, J., Muria-Gonzalez, M. J., Tran, P. N., Pettitt, A., et al. (2017) Functional genomics-guided discovery of a light-activated phytotoxin in the wheat pathogen *Parastagonospora nodorum* via pathway activation. *Environ Microbiol* **19**: 1975–1986.

Choquer, M., Lee, M.-H., Bau, H.-J., and Chung, K.-R. (2007) Deletion of a MFS transporter-like gene in *Cercospora nicotianae* reduces cercosporin toxin accumulation and fungal virulence. *FEBS Lett* **581**: 489–494.

Choquer, M., Dekkers, K. L., Chen, H.-Q., Cao, L., Ueng, P. P., Daub, M. E., and Chung, K.-R. (2005) The CTB1 gene encoding a fungal polyketide synthase is required for cercosporin biosynthesis and fungal virulence of *Cercospora nicotianae*. *Mol Plant Microbe Interact* **18**: 468–476.

Chumley, F. G., and Valent, B. (1990) Genetic analysis of melanin-deficient, nonpathogenic mutants of *Magnaporthe grisea*. *Mol Plant Microbe Interact* **3**: 135–143.

Chung, K.-R., and Liao, H.-L. (2008) Determination of a transcriptional regulator-like gene involved in biosynthesis of elsinochrome phytotoxin by the citrus scab fungus, *Elsinoë fawcettii*. *Microbiology* **154**: 3556–3566.

Collemare, J., Griffiths, S., Yuichiro, I., Karimi Jashni, M., Battaglia, E., Cox, R. J., and de Wit, P. J. G. M. (2014) Secondary metabolism and biotrophic lifestyle in the tomato pathogen *Cladosporium fulvum*. *PLoS One* **9**: e85877.

Crawford, J. M., and Townsend, C. A. (2010) New insights into the formation of fungal aromatic polyketides. *Nat Rev Microbiol* **8**: 879–889.

Daub, M. E., and Ehrenshaft, M. (2000) The photoactivated *Cercospora* toxin cercosporin: contributions to plant disease and fundamental biology. *Annu Rev Phytopathol* **38**: 461–490.

- Daub, M. E., Herrero, S., and Chung, K.-R. (2005) Photoactivated perylenequinone toxins in fungal pathogenesis of plants. *FEMS Microbiol Lett* **252**: 197–206.
- Daub, M. E., Herrero, S., and Chung, K. R. (2013) Reactive oxygen species in plant pathogenesis: the role of perylenequinone photosensitizers. *Antioxid Redox Signal* **19**: 970–989.
- de Jonge, R., Ebert, M. K., Huitt-Roehl, C. R., Pal, P., Suttle, J. C., Spanner, R. E., et al. (2018) Gene cluster conservation provides insight into cercosporin biosynthesis and extends production to the genus *Colletotrichum*. *Proc Natl Acad Sci USA* **115**: E5459–E5466.
- Demain, A. L., and Fang, A. (2000) The natural functions of secondary metabolites. In *History of Modern Biotechnology I*: Berlin, Heidelberg: Springer, pp. 1–39.
- Deng, H., Gao, R., Liao, X., and Cai, Y. (2017) Genome editing in *Shiraia bambusicola* using CRISPR-Cas9 system. *J Biotechnol* **259**: 228–234.
- Emms, D. M., and Kelly, S. (2015) OrthoFinder: solving fundamental biases in whole genome comparisons dramatically improves orthogroup inference accuracy. *Genome Biol* **16**: 157.
- Fajola, A. O. (1978) Cercosporin, a phytotoxin from *Cercospora* spp. *Physiol Plant Pathol* **13**: 157–164.
- Feng, B., Wang, X., Hauser, M., Kaufmann, S., Jentsch, S., Haase, G., et al. (2001) Molecular cloning and characterization of WdPKS1, a gene involved in dihydroxynaphthalene melanin biosynthesis and virulence in *Wangiella (Exophiala) dermatitidis*. *Infect Immun* **69**: 1781–1794.
- Finn, R. D., Attwood, T. K., Babbitt, P. C., Bateman, A., Bork, P., Bridge, A. J., et al. (2017) InterPro in 2017—beyond protein family and domain annotations. *Nucleic Acids Res* **45**: D190–D199.
- Foote, C. S. (1976) Photosensitized oxidation and singlet oxygen. *Free Radic Biol* **2**: 85–133.
- Frandsen, N. (1955) Untersuchungen über *Cercospora beticola*. *Verhalten des Pilzes in künstlicher Kultur Zucker* **8**: 451–456.
- Fujii, I., Mori, Y., Watanabe, A., Kubo, Y., Tsuji, G., and Ebizuka, Y. (1999) Heterologous expression and product identification of *Colletotrichum lagenarium* polyketide synthase encoded by the PKS1 gene involved in melanin biosynthesis. *Biosci Biotechnol Biochem* **63**: 1445–1452.
- Fujii, I., Yasuoka, Y., Tsai, H.-F., Chang, Y. C., Kwon-Chung, K. J., and Ebizuka, Y. (2004) Hydrolytic polyketide shortening by Ayg1p, a novel enzyme involved in fungal melanin biosynthesis. *J Biol Chem* **279**: 44613–44620.
- Fulton, T. R., Ibrahim, N., Losada, M. C., Grzegorski, D., and Tkacz, J. S. (1999) A melanin polyketide synthase (PKS) gene from *Nodulisporium* sp. that shows homology to the pks1 gene of *Colletotrichum lagenarium*. *Mol Gen Genet* **262**: 714–720.
- Gadd, G. M. (1982) Effects of media composition and light on colony differentiation and melanin synthesis in *Microdochium bolleyi*. *Trans Br Mycol Soc* **78**: 115–122.
- Gallo, A., Ferrara, M., and Perrone, G. (2013) Phylogenetic study of polyketide synthases and nonribosomal peptide synthetases involved in the biosynthesis of mycotoxins. *Toxins* **5**: 717–742.
- Guedes, R. C., and Eriksson, L. A. (2007) Photophysics, photochemistry, and reactivity: molecular aspects of perylenequinone reactions. *Photochem Photobiol Sci* **6**: 1089–1096.
- Hudson, J., Imperial, V., Haugland, R., and Diwu, Z. (1997) Antiviral activities of photoactive perylenequinones. *Photochem Photobiol* **65**: 352–354.
- Jenns, A., Daub, M., and Upchurch, R. (1989) Regulation of cercosporin accumulation in culture by medium and temperature manipulation. *Phytopathology* **79**: 213–219.
- Kauser, S., Schallreuter, K. U., Thody, A. J., Tobin, D. J., and Gummer, C. (2003) Regulation of human epidermal melanocyte biology by β -endorphin. *J Invest Dermatol* **120**: 1073–1080.
- Keller, N. P. (2015) Translating biosynthetic gene clusters into fungal armor and weaponry. *Nat Chem Biol* **11**: 671–677.
- Keller, N. P., and Hohn, T. M. (1997) Metabolic pathway gene clusters in filamentous fungi. *Fungal Genet Biol* **21**: 17–29.
- Keller, N. P., Turner, G., and Bennett, J. W. (2005) Fungal secondary metabolism—from biochemistry to genomics. *Nat Rev Microbiol* **3**: 937–947.
- Kroken, S., Glass, N. L., Taylor, J. W., Yoder, O. C., and Turgeon, B. G. (2003) Phylogenomic analysis of type I polyketide synthase genes in pathogenic and saprobic ascomycetes. *Proc Natl Acad Sci USA* **100**: 15670–15675.
- Langfelder, K., Streibel, M., Jahn, B., Haase, G., and Brakhage, A. A. (2003) Biosynthesis of fungal melanins and their importance for human pathogenic fungi. *Fungal Genet Biol* **38**: 143–158.
- Lendenmann, M. H., Croll, D., and McDonald, B. A. (2015) QTL mapping of fungicide sensitivity reveals novel genes and pleiotropy with melanization in the pathogen *Zymoseptoria tritici*. *Fungal Genet Biol* **80**: 53–67.
- Lendenmann, M. H., Croll, D., Stewart, E. L., and McDonald, B. A. (2014) Quantitative trait locus mapping of Melanization in the plant pathogenic fungus *Zymoseptoria tritici*. G3: Genes[Genomes]. *Genetics* **4**: 2519–2533.
- Liao, H.-L., and Chung, K.-R. (2008) Genetic dissection defines the roles of elsinochrome phytotoxin for fungal pathogenesis and conidiation of the citrus pathogen *Elsinoë fawcettii*. *Mol Plant Microbe Interact* **21**: 469–479.
- Liu, G. Y., and Nizet, V. (2009) Color me bad: microbial pigments as virulence factors. *Trends Microbiol* **17**: 406–413.
- Milat, M.-L., and Blein, J.-P. (1995) *Cercospora beticola* toxins III. Purification, thin-layer and high performance liquid chromatographic analyses. *J Chromatogr A* **699**: 277–283.
- Mistry, J., Finn, R. D., Eddy, S. R., Bateman, A., and Punta, M. (2013) Challenges in homology search: HMMER3 and convergent evolution of coiled-coil regions. *Nucleic Acids Res* **41**: e121–e121.
- Newman, A. G., and Townsend, C. A. (2016) Molecular characterization of the cercosporin biosynthetic pathway in the fungal plant pathogen *Cercospora nicotianae*. *J Am Chem Soc* **138**: 4219–4228.
- Oh, Y., Donofrio, N., Pan, H., Coughlan, S., Brown, D. E., Meng, S., et al. (2008) Transcriptome analysis reveals new insight into appressorium formation and function in

- the rice blast fungus *Magnaporthe oryzae*. *Genome Biol* **9**: R85.
- Perfect, S. E., Hughes, H. B., O'Connell, R. J., and Green, J. R. (1999) *Colletotrichum*: a model genus for studies on pathology and fungal–plant interactions. *Fungal Genet Biol* **27**: 186–198.
- Pihet, M., Vandeputte, P., Tronchin, G., Renier, G., Saulnier, P., Georgeault, S., et al. (2009) Melanin is an essential component for the integrity of the cell wall of *Aspergillus fumigatus* conidia. *BMC Microbiol* **9**: 177.
- Rohlf, M., and Churchill, A. C. L. (2011) Fungal secondary metabolites as modulators of interactions with insects and other arthropods. *Fungal Genet Biol* **48**: 23–34.
- Schumacher, J. (2016) DHN-melanin biosynthesis in the plant pathogenic fungus *Botrytis cinerea* is based on two developmentally regulated key enzyme (PKS)-encoding genes. *Mol Microbiol* **99**: 729–748.
- So, K.-K., Chung, Y.-J., Kim, J.-M., Kim, B.-T., Park, S.-M., and Kim, D.-H. (2015) Identification of a polyketide synthase gene in the synthesis of phleiochrome of the phytopathogenic fungus *Cladosporium phlei*. *Mol Cells* **38**: 1105–1110.
- Stergiopoulos, I., Collemare, J., Mehrabi, R., and De Wit, P. J. (2012) Phytotoxic secondary metabolites and peptides produced by plant pathogenic Dothideomycete fungi. *FEMS Microbiol Rev* **37**: 67–93.
- Stringlis, I. A., Zhang, H., Pieterse, C. M. J., Bolton, M. D., and de Jonge, R. (2018) Microbial small molecules – weapons of plant subversion. *Nat Prod Rep* **35**: 410–433.
- Talbot, N. J. (2003) On the trail of a cereal killer: exploring the biology of *Magnaporthe grisea*. *Annu Rev Microbiol* **57**: 177–202.
- Thompson, J. E., Fahnestock, S., Farrall, L., Liao, D.-I., Valent, B., and Jordan, D. B. (2000) The second naphthol reductase of fungal melanin biosynthesis in *Magnaporthe grisea*: tetrahydroxynaphthalene reductase. *J Biol Chem* **275**: 34867–34872.
- Tsai, H.-F., Wheeler, M. H., Chang, Y. C., and Kwon-Chung, K. J. (1999) A developmentally regulated gene cluster involved in conidial pigment biosynthesis in *Aspergillus fumigatus*. *J Bacteriol* **181**: 6469–6477.
- Tsuji, G., Kenmochi, Y., Takano, Y., Sweigard, J., Farrall, L., Furusawa, I., et al. (2000) Novel fungal transcriptional activators, Cmr1p of *Colletotrichum lagenarium* and Pig1p of *Magnaporthe grisea*, contain Cys₂His₂ zinc finger and Zn(II)₂Cys₆ binuclear cluster DNA-binding motifs and regulate transcription of melanin biosynthesis genes in a developmentally specific manner. *Mol Microbiol* **38**: 940–954.
- VanderMolen, K. M., Raja, H. A., El-Elimat, T., and Oberlies, N. H. (2013) Evaluation of culture media for the production of secondary metabolites in a natural products screening program. *AMB Express* **3**: 71.
- Weber, T., Blin, K., Duddela, S., Krug, D., Kim, H. U., Brucoleri, R., et al. (2015) antiSMASH 3.0—a comprehensive resource for the genome mining of biosynthetic gene clusters. *Nucleic Acids Res* **43**: W237–W243.
- Weiss, U., Merlini, L., and Nasini, G. (1987) Naturally occurring perylenequinones. In *Fortschritte der Chemie Organischer Naturstoffe / Progress in the Chemistry of Organic Natural Products*, Achenbach, H., Bhattacharyya, P., Chakraborty, D. P., Goto, T., Merlini, L., Nasini, G., and Weiss, U. (eds). Vienna: Springer Vienna, pp. 1–71.
- Wheeler, M. H., and Bell, A. A. (1988) Melanins and their importance in pathogenic fungi. In *Current Topics in Medical Mycology*, McGinnis, M. R. (ed). New York, NY: Springer New York, pp. 338–387.
- Williams, D. H., Stone, M. J., Hauck, P. R., and Rahman, S. K. (1989) Why are secondary metabolites (natural products) biosynthesized? *J Nat Prod* **52**: 1189–1208.
- Zhang, A., Lu, P., Dahl-Roshak, A. M., Pares, P. S., Kennedy, S., Tkacz, J. S., and An, Z. (2003) Efficient disruption of a polyketide synthase gene (pks1) required for melanin synthesis through *Agrobacterium*-mediated transformation of *Glarea lozoyensis*. *Mol Genet Genomics* **268**: 645–655.
- Zhang, H., Gao, S., Lercher, M. J., Hu, S., and Chen, W.-H. (2012) EvolView, an online tool for visualizing, annotating and managing phylogenetic trees. *Nucleic Acids Res* **40**: W569–W572.
- Zhao, N., Lin, X., Qi, S.-S., Luo, Z.-M., Chen, S.-L., and Yan, S.-Z. (2016) De novo transcriptome assembly in *Shiraia bambusicola* to investigate putative genes involved in the biosynthesis of hypocrellin A. *Int J Mol Sci* **17**: 311.
- Zhenjun, D., and Lown, J. W. (1990) Hypocrellins and their use in photosensitization. *Photochem Photobiol* **52**: 609–616.

Supporting Information

Additional Supporting Information may be found in the online version of this article at the publisher's web-site:

Fig. S1. Schematic DHN-melanin biosynthesis pathway of *M. oryzae*. In the first biosynthetic step, the PKS ALB1 forms 1,3,6,8-tetrahydroxynaphthalene (1,3,6,8-THN or T4HN) by ketide cyclization. Reduction by the tetrahydroxynaphthalene reductase 4HNR results in the formation of scytalone which will be dehydrated by RYS1, a scytalone dehydratase, to yield trihydroxynaphthalene (T3HN). The T3HN reductase BUF1 subsequently reduces T3HN to vermelone followed by a dehydration step mediated by RYS1 to form dihydroxynaphthalene (2HN), the immediate precursor of melanin.

Fig. S2. Agarose gel electrophoresis of PCR products confirming targeted gene replacements in *C. beticola* and *E. fawcettii* PKS knockout mutants as compared to wild type. (A) The site-directed integration of the hygromycin resistance cassette (*Hyg*) in the target gene for all mutants, amplified using a *Hyg*-specific reverse primer (Supporting Information Table 2, MDB-1145) and a gene-specific forward primer (MDB-1452, –1633, –1602 and –1607, respectively, from left to right). (B) The absence of the target gene in all mutants, amplified using gene-specific primer pairs (MDB-1253 and –1254, MDB-1726 and –1727,

MKE-179 and -180, MKE-177 and -178, respectively, from left to right). All PCR products were separated alongside the Invitrogen 1 Kb Plus DNA ladder (Thermo Fisher Scientific, Inc., Waltham) as a size reference.

Suppl. Table 1. List of the polyketide synthase (PKS) accession codes used in this study.

Suppl. Table 2. Primers used in this study.

Appendix S1: Supplementary Material.